Anal Bioanal Chem (2008) 391:433–441
DOI 10.1007/s00216-008-2001-4

ORIGINAL PAPER

Noninvasive and nondestructive NMR, Raman and XRF analysis of a Blaeu coloured map from the seventeenth century

K. Castro · S. Pessanha · N. Proietti · E. Princi · D. Capitani · M. L. Carvalho · J. M. Madariaga

Received: 23 January 2008 / Revised: 19 February 2008 / Accepted: 20 February 2008 / Published online: 29 March 2008

Abstract A complete multianalytical study of a hand-coloured map from the seventeenth century is presented. The pigments atacamite, massicot, minium, gypsum, carbon black and vermilion were determined by means of XRF and Raman spectroscopy. The state of conservation of the cellulosic support was monitored by means of unilateral NMR. The analysis was nondestructive and noninvasive, and thus several spectra were collected from the same areas, yielding more reliable results without damaging the artwork. The role of copper pigments in the oxidation processes observed in the cellulosic support is discussed, as well as the possible provenance of atacamite as a raw material instead of as a degradation product of malachite.

Keywords Raman · FTIR · NMR · Pigment · XRF · Cellulose · Degradation

K. Castro (✉) · J. M. Madariaga
Department Analytical Chemistry,
University of the Basque Country,
P.O. Box 644, 48080 Bilbao, Spain
e-mail: kepa.castro@ehu.es

S. Pessanha · M. L. Carvalho
Centro de Física Atómica da Universidade de Lisboa
Faculdade de Ciências,
Av. Prof. Gama Pinto 2,
1649-003 Lisboa, Portugal

N. Proietti · D. Capitani
Institute of Chemical Methodologies,
CNR, Research Area of Rome,
Via Salaria Km 29.300,
00016 Monterotondo Staz., Rome, Italy

E. Princi
Dipartimento di Chimica e Chimica Industriale,
University of Genova,
Via Dodecaneso 31,
16146 Genova, Italy

Introduction

New analytical methodologies and strategies recently developed in the field of cultural heritage have become a very important tool for studies of artworks, buildings of historical value and objects of archaeological interest.

Several authors have pointed out the suitability of combining various techniques to obtain different types of information about the objects being studied [1, 2]. This approach permits a complete study of the nature of the object if techniques providing molecular data are combined with other techniques providing elemental information. Moreover, the development of equipment that combines two or more different techniques in the same system is now commonplace. Spectroscopic techniques are very suitable for this purpose, and it is now possible to find hybrid instruments such as Raman–SEM–EDX (which has not yet been applied to cultural heritage), Raman–LIBS [3], Raman–XRF [4] and Raman–IR [5].

However, some problems may arise during the studies of some artworks, buildings and archaeological objects that must be carried out in the field because sampling is not possible. The above mentioned hybrid instruments are difficult to move and are commonly used within the laboratory. However, many portable systems allowing nondestructive and noninvasive in situ investigations are readily available. These systems have produced very reliable performances when they have been applied to the analysis of cultural heritage objects. Because these systems allow nondestructive investigations to be performed directly on the artwork, it is possible to carry out as many analyses as are needed, resulting in more reliable results. A comparison of several portable Raman systems has been recently published [6], and several examples of the applications of these new systems can be found in the literature [7–10].

In the framework of the Papertech project (financed by the European Commission), a multianalytical approach was selected in order to perform a diagnostic analysis of artworks on paper support. This approach makes use of noninvasive portable equipment such as Raman microprobe spectroscopy, micro X-ray fluorescence (μXRF) and nuclear magnetic resonance (NMR). In this work, a full noninvasive and nondestructive study of a map from the seventeenth century is presented.

Raman spectroscopy has been applied to different types of artworks [11, 12]. Using this technique it is possible to characterise all of the inorganic pigments and materials present in these art objects. In addition, in the case of artworks on paper supports, the presence of fillers in the cellulose can be detected. Moreover, the sensitivity of this technique allows also the degradation mechanisms of some cultural heritage materials to be determined [13].

It is possible to find some interesting recent applications of XRF to the analysis of artworks in the literature [14, 15]. XRF provides the elemental compositions of the objects under analysis and it can be used as a perfect complementary technique to molecular techniques such as Raman spectroscopy. Several recent reviews can be found in the literature that summarise the most important applications of XRF to artwork studies, conservation and restoration [16, 17], proving the suitability of this technique for nondestructive analysis.

In the last few years a completely noninvasive NMR instrument has been developed within the framework of a European Project (Eureka Project Σ!2214- *Eurocare Mouse*). Using this equipment, sampling can be avoided by positioning the sensor near the intact object at different positions. This apparatus is portable, completely noninvasive and suitable for studying cultural heritage items [18–20]. Using this instrumentation, important NMR parameters such as the spin-lattice relaxation time T_1 and the spin-spin relaxation time T_2 can be measured [21]. The spin-spin relaxation time is one of the most sensitive NMR parameters, and it allows paper in a good state of preservation to be distinguished from degraded paper [8, 22].

Specimen

The artwork analysed was a map from the Italian region of Vicenza made on handcrafted paper using the technique known as etching engraving (black ink). In this case, the map was also illuminated (painted) by hand in several colours. This map was part of one of the most important atlases from the seventeenth century, the *Atlas Major*.

Willem Janszoon Blaeu (1571–1638) and his son Joan Blaeu (1596–1673) were the most widely known cartographic publishers of the seventeenth century. In 1630 Blaeu purchased 37 plates of the Mercator Atlas, added them to his own collection and published the *Atlantis Appendix*, which contained 60 maps. By 1635 he issued the first two volumes of his planned world atlas, *Atlas Novus* or the *Theatrum Orbis Terrarum*. In 1638 Willem died and it was under the control of Joan that the Blaeu printing press achieved lasting fame in Europe in the seventeenth century. Joan completed his father's grand project in 1655 with the sixth and final volume of the *Atlas Novus*.

By 1662 the atlas had grown to 11 or 12 volumes depending on the edition and the inclusion of a sea atlas. At this time the atlas became known as the *Atlas Major*. This atlas was the most expensive printed book of the seventeenth century (it cost 460 florins, equivalent to about 20,000 Euros), consisting of nearly 600 double-page maps and 3000 pages of text. The maps were richly embellished, often hand-coloured and heightened with gold. This period is known as the Golden Age of Cartography. Recognising that the wealthy patrons who would buy such atlases were primarily interested in display, aesthetic considerations such as luxury bindings, fine engraving, bright colours and beautiful typography were emphasised. How up-to-date the maps was considered less important.

It is thought that 1300 issues were published in the first edition. In 1993, 129 issues written in Latin had survived, 84 issues in French, 59 issues in Dutch and 45 issues in Spanish. Original maps are rare collectors' items that are still sold today [23].

The map (415×494 mm) of the territory of Vicenza (Italy) was published in one of the volumes in 1640. This map is in a poor state of preservation due to oxidation processes (resulting from the presence of some green colours), loss of support, scratches, tears, etc. In some areas on the backside of the map several adhesive strips are also present and have promoted the oxidation of the paper support. The polychromy is in a relatively good state of conservation, but the inks seem to have faded.

Experimental

Raman and X-ray fluorescence (XRF) spectroscopies were used for pigment and filler analysis. The Raman system consisted of a Renishaw (Wotton-under-Edge, UK) RA100 system coupled to a microprobe (785 nm excitation laser, CCD detector). Neutral density filters (1% and 10%) implemented in the system were used to attenuate the laser power on the samples. The head of the microprobe implemented a 20× enlargement objective as well as a microvideo camera that was focussed on the area under analysis.

For XRF analysis, portable micro-XRF equipment was used. The instrument consisted of molybdenum (Mo) anode

X-ray tube working at a maximum voltage/current of 50 kV/0.6 mA and using a special Xflash SDD detector (5 mm^2) with a 2×25 μm helium -illed beryllium window (energy resolution was <155 eV at 10 kcps with a max. count rate of >100 kcps). The X-rays were collimated by a tantalum collimator with a diameter of 0.65 mm. The measuring head of the equipment implemented a CCD camera that could be focussed onto the sample using a motorised XYZ positioning unit controlled by the computer. The measurements were carried out while maintaining the maximum voltage/current for 1000 s. As Raman and XRF enable completely nondestructive analyses to be performed directly over the samples without any kind of sampling, several analyses were done in different areas of the same shade in order to obtain reliable results.

A nonportable spectrometer was also used in this work for quantitative EDXRF analysis. This system consisted of a commercial X-ray tube (PW 1140, 100 kV, 80 mA, maximum) equipped with a Mo changeable secondary target. Using this system it was possible to obtain a monochromatic source with the K_α and K_β lines of Mo (17.44 and 19.60 keV, respectively). The X-ray tube, the secondary target and the sample were positioned in a triaxial geometry, thus decreasing the background [24]. Both the X-ray beam emitted by the secondary target and the sample were collimated throughout two silver apertures in order to reduce the scattered radiation and improve the detection limits. The system implemented a Si(Li) detector (energy resolution was 135 eV at 5.9 keV), with a 30 mm^2 active area and an 8 μm beryllium window. The operating conditions of this system for all analysed spectra were 50 kV and 20 mA. Quantification was achieved through the fundamental parameters method [25].

Finally, the state of preservation of the paper support was evaluated by means of nuclear magnetic resonance (NMR). NMR measurements were performed with a commercial unilateral NMR "ProFiler" from Bruker Biospin (Milan, Italy). The magnetic field was generated using two anti-parallel permanent magnets mounted on an iron yoke with the radiofrequency (RF) coil positioned in the gap. The probe, operated at 18.153 MHz, had a penetration depth of about 0.5 mm inside the sample.

The maximum echo signal, corresponding to a π/2 pulse, was obtained with a pulse width of 3 μs, and the dead time was less than 15 μs. Spin-lattice relaxation times were measured with the aperiodic saturation recovery sequence according to a previously published procedure [21]. Spin-spin relaxation times were measured with the CPMG sequence according to a previously published procedure [8]; 1024 echoes were recorded, and the time between the 90° and 180° degree pulses was 50 μs. The intensity of the proton signal was measured by performing single Hahn echo measurements with an echo time of 12 μs.

Results and discussion

A full analysis of the map was carried out. This included completely characterising the support by studying the condition of the cellulose, and identifying all of the fillers and pigments used to embellish the map.

Identification of the support

It is clear, based on the Raman spectrum obtained, that the support of the map is cellulose, with characteristic bands located at 1118 cm^{-1} (C–O–C of the α-glycosidic linkage of hemicellulose) and 1092 cm^{-1} (C–O–C of the β-glycosidic linkage of cellulose and hemicellulose), among others.

Evaluation of cellulose

The T_1 spin-lattice relaxation times were measured on a few selected points of the map, which were labelled with their x,y coordinates (Fig. 1, left). T_1 values measured on the white border ($T_1 = 154 \pm 20$ms), as well as in the point ($7,4\ T_1 = 159 \pm 20$ms) are characteristic values for ancient paper. Nevertheless, T_1 values obtained in points ($27,4\ T_1 = 73 \pm 3$ms), ($16,21\ T_1 = 109 \pm 9$ms) and ($45,21\ T_1 = 86 \pm 5$ms) are definitely shorter than those measured on the border. This shortening is possibly due to the presence of paramagnetic impurities that act as relaxation centres. Accordingly, XRF analysis of the support revealed the presence of a significant amount of Cu and Fe. It is well known that the presence of these impurities, which are essentially transition metal ions, may affect the kinetics of paper hydrolysis, since they act as catalysts.

The T_2 spin-spin relaxation time is more sensitive to the degradation of paper than T_1, whereas T_1 is more sensitive to the presence of paramagnetic impurities that may occur in the ink. Because T_1 measurements are rather long and the authors were more interested in the degradation occurring in the cellulose, a systematic T_2 study of the map was carried out, whereas only a few T_1 measurements were performed.

T_2 spin-spin relaxation time measurements were performed at the points of the (x,y) grid reported on the map (see Fig. 1, right). In Fig. 2, the T_2 relaxation times measured at the "x" position on the grid are reported. It is worth noting that the T_2 values are, on average, rather short (about 0.3 ms), except for those measured at the points (25, 7), (27, 7), (25, 9) and (27, 9), which are significantly longer. An average T_2 value of as little as 0.3 ms is a typical value observed for aged ancient paper. The longer T_2 values measured at the points (25, 7), (27, 7), (25, 9) and (27, 9) are possibly due to the presence of organic substances used in old restoration procedures (from the glue of adhesive strips on the back of the map for example). Note that the same trend was also observed for the intensity

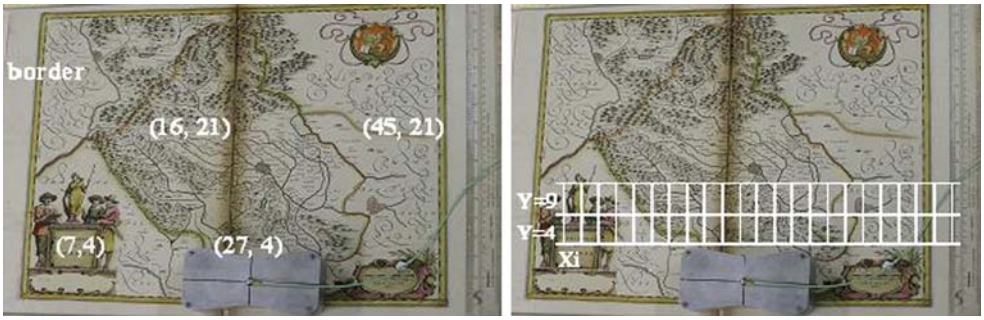

Fig. 1 *Left*: points on the map at which T_1 relaxation times were measured. *Right*: points on the map at which T_2 relaxation times were measured. The probe head used for the measurements is also shown

of the Hahn echo signal versus the "x" position of the grid (Fig. 3).

Filler detection

The Raman and XRF analysis of this artwork highlighted several important features. For example, the Raman analysis of the support showed that gypsum ($CaSO_4.2H_2O$) was used as a filler in the cellulose (bands at 1008 cm^{-1}). Moreover, XRF analysis confirmed the results obtained by Raman spectroscopy, since it detected large quantities of calcium and sulfur in the support, resulting from the gypsum. However, alkaline reserve does not seem to have been added to the cellulose (a Raman signal was not found at 1085 cm^{-1}). This omission has influenced the stability of the support, which appears quite degraded and oxidised.

Pigment characterisation

Pigment characterisation was done according to the methodology followed in previous works [13]. This methodology consists of screening the elements present in the colours using portable, noninvasive XRF systems. Afterwards, the colours are analysed by a noninvasive Raman system in order to ascertain the molecular compositions of the pigments; that is, how the elements determined by XRF are linked. In this case, in order to test the performance of the portable equipment, a nonportable XRF system was also used for quantitative analysis. Measurements of the decorated zone on a page map can be influenced by the decoration of the other side of the page. However, in this case only one of the sides was decorated.

In the different red areas on the map, XRF analysis showed the presence of high levels of lead and mercury, indicating the presence of vermilion and lead pigments (see Table 1). Unfortunately, elemental analysis techniques cannot determine which lead pigments are present.

In all cases, Raman analysis confirmed the presence of minium (Raman bands at 549, 477, 456, 390, 313 and 226 cm^{-1}) and vermilion (343, 285 and 253 cm^{-1}) [26] in different proportions (see Fig. 4). Surprisingly, in some cases spectral bands due to the presence of lead yellow oxide (massicot, PbO) were detected (located at 383 and 286 cm^{-1}). The reason for the presence of PbO in the red regions is not clear, but according to the literature [27] the colour of minium can be obtained by burning lead white or massicot. Thus, the presence of PbO could be linked to the manufacture of minium pigment. However, it is more probable that the manufacturer added this pigment to obtain the desirable shadow. In fact, the red jacket presents a yellowish shade and the Raman signal from PbO in this region is more clear and intense than in the other red areas.

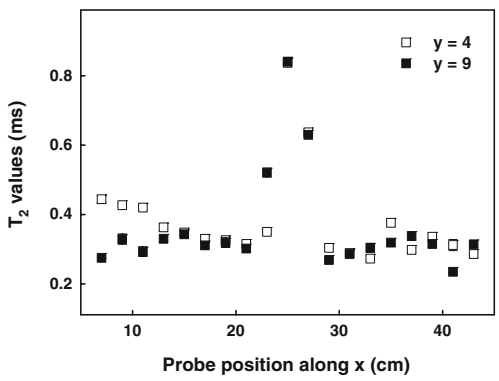

Fig. 2 T_2 spin-spin relaxation times versus the "x" position (probe position) on the grid

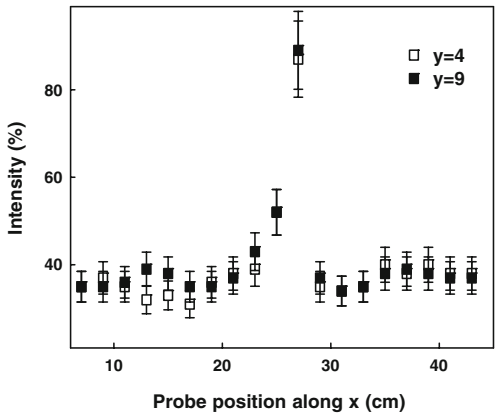

Fig. 3 Intensity of the Hahn echo versus the "x" position (probe position) on the grid

Table 1 Mean elemental concentrations and standard deviations (μg g^{-1}) obtained with the EDXRF spectrometer for the paper and some pigmented areas

Element	Paper	Green symbol	Green trousers	Green jacket	Red jacket	Yellow lion	Red symbol
	Mean±SD	Mean±SD	Mean±SD	Mean±SD	Mean±SD	Mean±SD	Mean±SD
K	1200±520	990±20	2700±20	2600±300	3300±1000	700±20	2000±350
Ca	1640±730	960±20	2200±10	2900±100	1600±510	910±20	2900±370
Fe	130±10	140±10	600±10	590±20	290±90	120±4	480±270
Cu	160±10	6300±300	32000±200	29000±400	290±100	200±25	470±300
Zn	24±5	30±13	BDL	BDL	BDL	BDL	BDL
As	BDL	BDL	BDL	60±10	BDL	BDL	BDL
Hg	BDL	BDL	BDL	BDL	620±140	BDL	600±500
Pb	57±3	120±5	5500±10	1900±100	53000±12000	13000±900	130000±13000
Cl	4000±1000	1300±200	4000±100	11000±1000	134000±65000	230000±160000	1900±200

In contrast, in the red roofs and in the red medallion (the areas that present the deepest shades of red), the signals from PbO are weak. In addition, Raman bands due to the presence of lead sulfate appear in the spectrum (band at 978 cm^{-1}). It seems that the presence of lead sulfate is associated with the presence of high quantities of red vermilion. However, lead sulfate was not found in the red areas of the red jacket, and so the different red areas seem to be painted with pigments or colours of different qualities. Finally, in the shadows of the man's red jacket, carbon black was also found (broad bands located at 1600 and 1330 cm^{-1}).

For the green-coloured areas, XRF analysis showed a high quantity of copper in all cases, denoting the presence of a green or blue copper pigment. This element appeared together with lead in the green trousers and jacket (see Fig. 5) and with iron in the case of the green socks. In contrast, the green medallion on the right at the bottom of the map was dominated by copper with a very low concentration of lead (see Table 1).

The Raman analysis of the same green areas showed very interesting and surprising results. On the one hand (see Fig. 6), the most important bands seen in the spectrum of the green jacket are due to the presence of atacamite ($Cu_2Cl(OH)_3$); these bands were found at 974, 910, 819 and 510 cm^{-1} (in the spectra these bands are very weak). The presence of this compound is unusual but not strange. In fact, some authors state that this pigment is a consequence of the degradation of other pigments such as malachite or azurite [28, 29]. In contrast, other authors maintain that old masters knew of this pigment [30]. The chlorine (Cl) detected by the XRF spectrometers may have come from the atacamite or it could have been a degradation product from another green pigment resulting from the impact of chloride salts. Unfortunately, in the other green areas Raman analysis did not provide any information on the green pigments (this fact will be discussed further below).

In the green jacket, atacamite was found to be mixed with massicot (bands at 383 and 286 cm^{-1}). Furthermore, using the camera implemented in the head of the probe, it

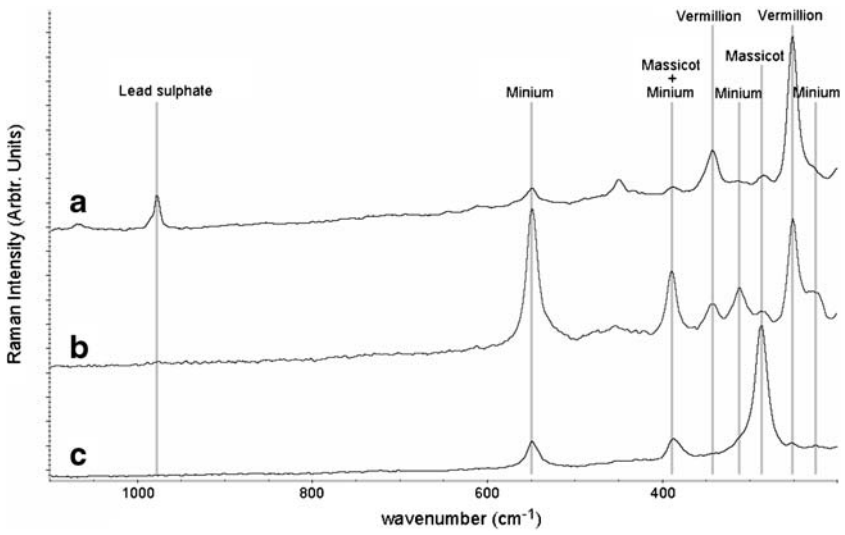

Fig. 4 Raman spectra of some of the red areas analysed: (**a**) red roof, (**b**) red medallion and (**c**) red jacket

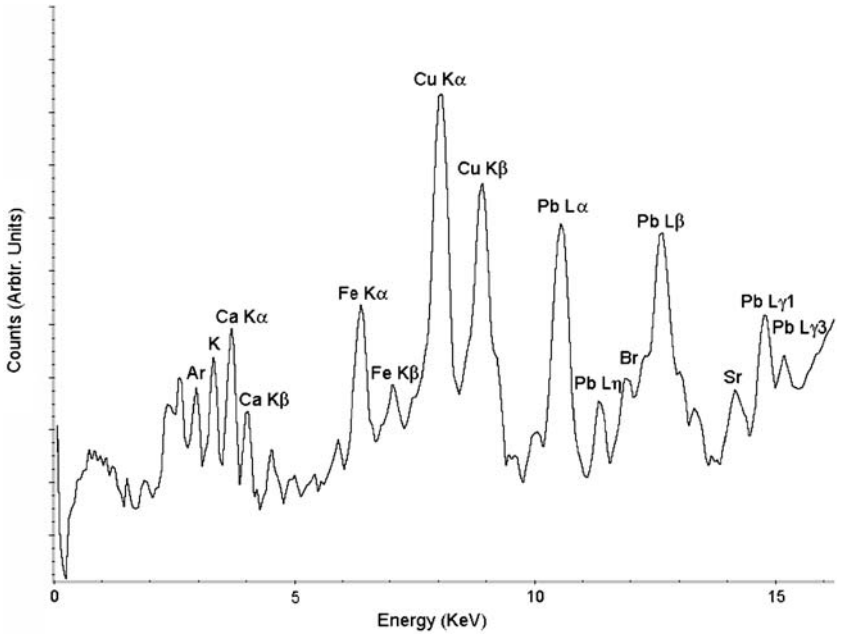

Fig. 5 Spectrum obtained with EDXRF equipment for the green jacket

was possible to clearly distinguish the green and the yellow grains. In some of the spectra from the other green areas, a weak band at 286 cm^{-1} due to the presence of massicot could be found.

As mentioned above, copper and iron were determined in the green sock of one of the men. These probably arose from a yellow iron oxide and an undetermined copper pigment. However, Raman analysis of this area did not reveal the presence of any band from any pigment. The same happened during the Raman analysis of the green medallion, where no signal was found. It is clear that a copper pigment is present, but it was not possible to determine it.

XRF analysis of the pink-coloured areas did not reveal the meaningful presence of any element over the background. Surprisingly, during the Raman analysis both minium and vermilion were determined in this area. Nevertheless, only a few little grains of these pigments could be seen through the TV camera, and so their presence could be due to contamination. No other Raman signal was obtained from this colour, meaning that an organic pigment could be responsible for the pink colour.

In the yellow colour of the woman, lead was detected by XRF (see Fig. 7) together with arsenic (As). However, the As is only present in very small amounts (70±10 μg/g), whereas the concentration of Pb reaches 3500 μg/g. The high Pb concentration might suggest the use of lead tin yellow (Pb_2SnO_4), Naples yellow ($Pb_3(SbO_4)_2$), or massicot (PbO). Arsenic is usually found together with lead as a

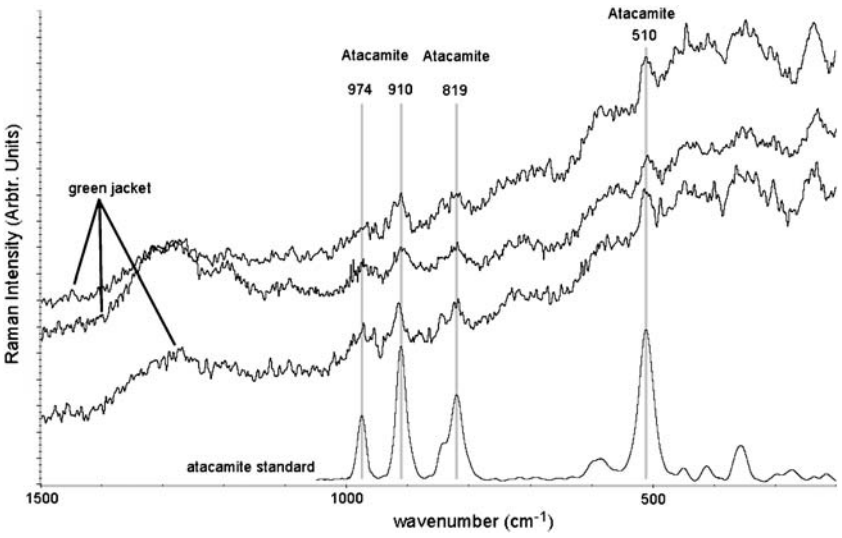

Fig. 6 Raman spectra of the different green areas analysed. The standard spectrum of atacamite is shown at the *bottom*. Three different points on the green jacket where atacamite was found are shown at the *top*

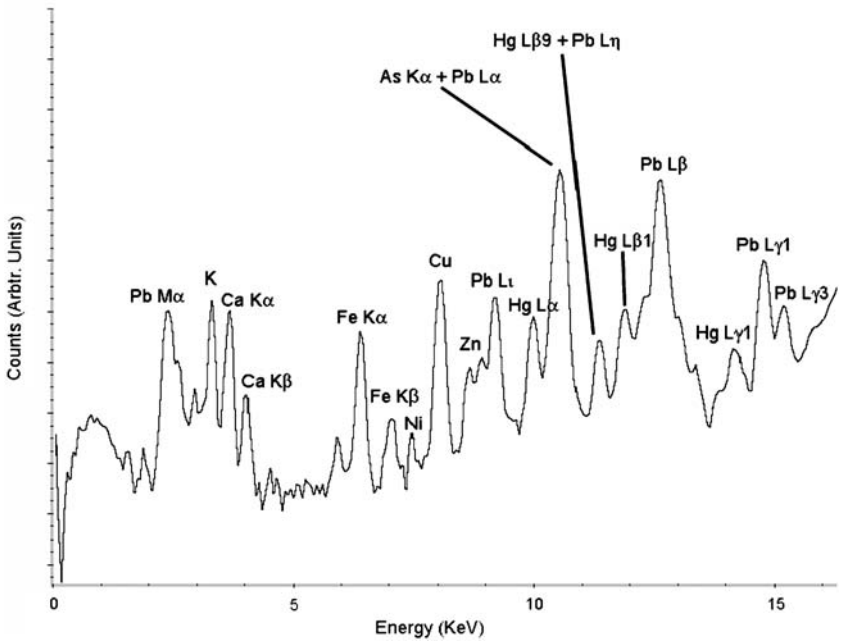

Fig. 7 Spectrum obtained with EDXRF equipment for the yellow colour

trace element, and this could explain its presence. Considering that neither Sn nor Sb were found, this pigment is proposed to be massicot. This suggestion was corroborated by Raman analysis (very weak bands at 290 cm^{-1} from PbO).

Finally, the Raman spectrum of the black ink of the etching engraving shows a band due to the presence of a carbon black pigment, which presents two characteristic broad bands at 1600 and 1330 cm^{-1}.

Atacamite as raw material

It is clear that the green areas are completely degraded based on the state of the cellulose support, which is oxidised. The effects of copper pigments are common knowledge [31], as are those of polysaccharides and monosaccharides with free glucoside hydroxyl groups, which react easily with Cu^{2+}. The result of this reaction is the breakdown of sugars to simple organic acids which destroy both the binder and the paper. The reaction takes place under very humid conditions. The decay of the copper green pigments as well as the destruction caused by them to artworks on paper support has been reported elsewhere [32]. This fact could be the reason for the absence of Raman bands from some of the green areas (the pigment is decayed and no Raman signal can be obtained) as well as the low intensity of the bands from the atacamite, which could be partially decayed (this pigment is also a poorly scattering material under the 785 nm laser).

Unfortunately, the confusion and lack of literature about atacamite pigment mean that we cannot assess whether this pigment was used as a raw material or whether it is a degradation product. This pigment has been determined in many artworks as a corrosion product of bronze artifacts, but in other artworks (manuscripts, etc.), no conclusions are made regarding its provenance, even though atacamite is supposed to be a degradation product in some cases.

In this case, however, the presence of a significant amount of chlorine all over the map could at first sight suggest that the atacamite is a degradation product from other green or blue copper pigments such as malachite or azurite (very common pigments during the seventeenth century). Moreover, this degradation could be due to an attack of saline weathering. Vandenabeele et al. [33] report a degradation process of malachite to polymorphs of copper(II) hydroxychlorides in the presence of chloride and humidity. Frost [34] takes this further to propose a degradation pathway from malachite to polymorphs of copper hydroxychlorides.

Nevertheless, taking into account the quantitative results of XRF analysis (see Table 1), it is possible to establish that the molar relationship between copper and chlorine (Cu:Cl) for the area where atacamite is found is approximately 2:1; that is, the same molar relationship as occurs in atacamite ($Cu_2Cl(OH)_3$). Thus, it is possible to conclude that atacamite was used as a raw material.

In contrast, this relationship is far from that found for the atacamite in the other areas. In fact, no signal from this pigment or from any other green copper material could be seen, and thus no conclusion can be made about which pigment was used in these green areas. However, it is possible to state that atacamite was not used, that the original pigment is completely degraded and that it is responsible for the oxidation-based decay of the cellulose.

Conclusions

In this work, the complementarity of noninvasive and nondestructive micro-XRF, NMR and micro-Raman analysis has been demonstrated by studying the materials present in an artwork (pigments and fillers). The proposed approach makes use of elemental composition information as well as molecular information. In this way, the assignment of Raman signals is more reliable, and it is possible to ensure that all elements are related to a pigment or material, and so all materials are determined in an elemental and molecular way.

However, when a specimen is analysed by Raman spectroscopy it is sometimes difficult to ensure that all pigments and materials present in the artwork have been identified by this technique, due to low scattering properties, fluorescence phenomena, etc. If elemental analysis is skipped, the results are incomplete. To overcome this problem, the combination of Raman spectroscopy with XRF analysis is presented here as a good compromise. That is, even if Raman spectra cannot be obtained, the elemental composition can still provide important clues about the materials. This was the case with some of the green pigments analysed during this work.

In addition, the cellulosic support was also successfully evaluated and characterised by means of the abovementioned techniques and NMR. Nuclear magnetic resonance provides very valuable information about the state of conservation of the cellulosic support. Furthermore, due to the shortening of the T_1 relaxation times, it can also determine the presence of paramagnetic impurities (Cu, Fe) which can act as catalysts in the cellulose degradation. These impurities were also detected by means of XRF, and the results from XRF confirmed all of the results obtained by NMR.

One of the most important features of the present work is the use of nondestructive and noninvasive techniques. These techniques have become very important in the field of cultural heritage because they do not require sampling and the artworks are not damaged during analysis. The portable and nonportable XRF results indicate that both systems presented the same results of qualitative analysis. However, the nonportable XRF system posed some problems when analysing very small coloured areas since the spot of the beam is quite large and the system was not able to focus on just one colour, so the signal related to the selected areas plus the surrounding areas. In contrast, the mobile XRF system has a better spatial resolution and the laser beam was small enough to perform the analysis of very small areas (less than 100 μm).

However, a nonportable XRF analyser is still irreplaceable for quantitative analysis. This system is more stable when focusing on the selected area and the size of the beam ensures that the mean concentration obtained for the area under analysis is accurate. In contrast, the small spot size resulting from the small diameter of the beam in the portable XRF system means that the average concentration of the area obtained using this system is not guaranteed to be accurate, which in turn means that only a semi-quantitative analysis can be performed with this system.

Acknowledgements This work was partially funded by the European Project PAPERTECH (INCO-CT-2004–509095). Dr. K. Castro is grateful to the Ministry of Education and Science for his contract at the UPV/EHU (PTA 2003–02–00050). Authors would like to thank Prof. Enrico Pedemonte and Prof. Ezio Martuscelli for the support, the suggestions and the fruitful discussions.

References

1. Shen AG, Wang XH, Xie W, Shen J, Li HY, Liu ZA, Hu JM (2006) J Raman Spectrosc 37:230–234
2. Benedetti D, Alessandri I, Bergese P, Bontempi E, Colombi P, Garipoli D, Pedrazzani R, Zanola P, Depero LE (2006) Microchim Acta 155:101–104
3. Giakoumaki A, Osticioli I, Anglos D (2006) Appl Phys A 83:537–541
4. Andrikopoulos KS, Daniilia S, Roussel B, Janssens K (2006) J Raman Spectrosc 37:1026–1034
5. Adar F, IeBourdon G, Reffner J, Whitley A (2003) Spectroscopy 18:34–40
6. Vandenabeele P, Castro K, Hargreaves M, Moens L, Madariaga JM, Edwards HGM (2007) Anal Chim Acta 588:108–116
7. Pérez-Alonso M, Castro K, Madariaga JM (2006) Anal Chim Acta 571:121–128
8. Proietti N, Capitani D, Pedemonte E, Blümich B, Segre AL (2004) J Magn Reson 170:113–120
9. Papageorgiou I, Liritzis I (2007) Archaeometry 49:795–813
10. Perez-Arantegui J, Resano M, Garcia-Ruiz E, Vanhaecke F, Roldan C, Ferrero J, Coll J (2008) Talanta 74:1271–1280
11. Castro K, Vandenabeele P, Rodríguez-Laso MD, Moens L, Madariaga JM (2004) Anal Bioanal Chem 379:674–683
12. Ferrer N, Vila A (2006) Anal Chim Acta 555:161–166
13. Castro K, Pérez-Alonso M, Rodríguez-Laso MD, Etxebarria N, Madariaga JM (2007) Anal Bioanal Chem 387:847–860
14. Manso M, Costa M, Carvalho ML (2007) Nucl Instrum Methods A 580:732–734
15. Manso M, Carvalho ML (2007) J Anal Atom Spectrom 22:164–170
16. Lindgren ES (2000) X-Ray Spectrom 29(1):1–129 (special Issue on applying X-ray spectrometry to cultural heritage)
17. Schreiner M, Fruhmann B, Jembrih-Simburger D, Linke R (2004) Powder Diffr 19:3–11
18. Blümich B, Anferova S, Sharma S, Segre AL, Federici C (2003) J Magn Reson 161:204–209
19. Proietti N, Capitani D, Cozzolino S, Valentini M, Pedemonte E, Princi E, Vicini S, Segre AL (2006) J Phys Chem B 110:23719–23728
20. Proietti N, Capitani D, Rossi E, Cozzolino S, Segre AL (2007) J Magn Reson 186:311–318
21. Capitani D, Segre AL, Attanasio D, Blicharska B, Focher B, Capretti G (1996) Tappi J 79:113–122
22. Capitani D, Emanuele MC, Segre AL, Fanelli C, Fabbri AA, Attanasio D, Focher B, Capretti G (1998) Nord Pulp Pap Res J 13:95–100
23. Keuning J (1973) In: Donkersloot-De Vrij YM (eds) Willem Jansz Blaeu: a biography and history of his work as a cartographer and publisher. Theatrum Orbis Terrarum Ltd., Amsterdam
24. Magalhães T, von Bohlen A, Carvalho ML, Becker M (2006) Spectrochim Acta B 61:1185–1193

25. Manso M, Pessanha S, Carvalho ML (2006) Spectrochim Acta B 61:922–928
26. Castro K, Perez-Alonso M, Rodriguez-Laso MD, Fernandez LA, Madariaga JM (2005) Anal Bioanal Chem 382:248–258
27. Gettens RJ, Kühn H, Chase WT (1997) Lead white. In: Roy A (ed) Artists' pigments: a handbook of their history and characteristics, vol 2. Oxford University Press, Oxford
28. Eremin K, Stenger J, Green ML (2006) J Raman Spectrosc 37:1119–1124
29. Frost RL, Martens W, Kloprogge JT, Williams PA (2002) J Raman Spectrosc 33:801–806
30. Lepot L, Denoel S, Gilbert B (2006) J Raman Spectrosc 37:1098–1103
31. Kühn H (1997) Verdigris and copper resinate. In: Roy A (ed) Artists' pigments: a handbook of their history and characteristics, vol 2. Oxford University Press, Oxford
32. Castro K, Sarmiento A, Princi E, Pérez-Alonso M, Rodríguez-Laso MD, Vicini S, Madariaga JM, Pedemonte E (2007) Trend Anal Chem 26:347–359
33. Vandenabeele P, Lambert K, Matthys S, Schudel W, Bergmans A, Moens L (2005) Anal Bioanal Chem 383:707–712
34. Frost RL (2003) Spectrochim Acta A 59:1195–1204